Characteristics of the viscous superlayer in shear free turbulence and in planar turbulent jets

Rodrigo R. Taveira and Carlos B. da Silva

Citation: Physics of Fluids (1994-present) **26**, 021702 (2014); doi: 10.1063/1.4866456
View online: http://dx.doi.org/10.1063/1.4866456
View Table of Contents: http://scitation.aip.org/content/aip/journal/pof2/26/2?ver=pdfcov
Published by the AIP Publishing

PHYSICS OF FLUIDS **26**, 021702 (2014)

Characteristics of the viscous superlayer in shear free turbulence and in planar turbulent jets

Rodrigo R. Taveira and Carlos B. da Silva[a)]
IDMEC/Instituto Superior Técnico, University of Lisbon, Pav. Mecânica I, 1º andar/esq./LASEF, Av. Rovisco Pais, 1049-001 Lisboa, Portugal

(Received 26 October 2013; accepted 6 February 2014; published online 24 February 2014)

Direct numerical simulations of a planar jet and of shear free turbulence at $Re_\lambda = 115$–140 using very fine resolutions allow the first direct identification and characterisation of the viscous superlayer (VSL) that exists at the edges of mixing layers, wakes, jets, and boundary layers, adjacent to the turbulent/non-turbulent interface. For both flows the VSL is continuous with higher local thicknesses forming near the larger intense vorticity structures. The mean thickness of the VSL is of the order of the Kolmogorov micro-scale and agrees well with an estimate based on the Burgers vortex model. © *2014 AIP Publishing LLC*. [http://dx.doi.org/10.1063/1.4866456]

In turbulent free shear flows such as jets, wakes, and mixing layers, and in turbulent boundary layers a sharp interface which is continually deformed over a wide range of scales separates the turbulent from the irrotational flow region: the turbulent/non-turbulent interface (TNTI).[1] Exchanges of mass, momentum, and scalars (heat) take place across this interface, which makes their study very important to many engineering and geophysical flows, e.g., the flow dynamics near the TNTI governs the entrainment and mixing rates in turbulent reacting jets.

Probably the most distinctive feature of the TNTI consists in the characteristic (sharp) vorticity jump that is observed linking the irrotational to the turbulent flow regions, as shown in conditional statistics in respect to the distance from the TNTI.[1–3] Several works[2,4] have shown that this sharp vorticity rise is largely an inertial/inviscid effect caused by the dominating effect of vorticity production by vortex stretching. This vorticity jump defines the so called *turbulent sublayer* (TSL) region[5] with thickness δ_ω whose scaling is imposed by the nearby eddy structure.[5,8]

A related longstanding question regarding these interfaces concerns the existence of a *laminar or viscous superlayer* (VSL) responsible by the transfer of vorticity from the core of the turbulent region into the irrotational flow region by viscous diffusion. The VSL forms the outer sublayer of the TNTI.[1] The existence of this layer was first suggested by Corrsin and Kistler[6] more than half a century ago, but until now no direct evidence (i.e., visualisation) of this layer has been reported, either from numerical simulations or experimental data.[3] Consequently, the characteristics of this layer, e.g., its geometry, kinematics, and dynamics remain largely unexplored. This layer must exist, they argued, because the only mechanism that can generate the growth or vorticity in a medium which is initially depleted of vorticity is vorticity diffusion.[7] The mean thickness of the VSL $\langle\delta_\nu\rangle$ was estimated by Corrsin and Kistler[6] to be of the order of the Kolmogorov micro-scale with the following reasoning: since the physical process within this layer is the viscous diffusion of vorticity from the turbulent core into the irrotational region, this process should be solely controlled by the amount of vorticity in the turbulent region ω' and by the molecular viscosity ν. On dimensional grounds it follows that the characteristic length scale for this process, defined as the thickness of the VSL, is $\delta_\nu = \delta_\nu(\nu, \omega')$, leading to $\delta_\nu \sim (\nu/\omega')^{1/2} \sim (\nu^3/\varepsilon)^{1/4} \sim \eta$, where ε is the mean rate of viscous dissipation in the core of the turbulent region.

The goal of the present work is to identify the VSL and investigate its geometrical aspects such as its continuity, length, thickness and location, and its relation to the eddy structure from the

a)E-mail: carlos.silva@tecnico.ulisboa.pt

TSL. The present work presents the first direct observation of the VSL which became accessible due the particularly fine direct numerical simulations (DNS) used here, and to a clear mathematical definition of the VSL. The simulations were already used by the authors in several previous works[8,9] and therefore only a short description will be given here. The simulations use a Navier-Stokes solver employing pseudo-spectral methods for spatial discretization and a 3rd order, 3 step Runge-Kutta scheme for temporal advancement and were fully dealiased using the 2/3 rule.

The first simulation consists in shear free turbulence (SFT) in a periodic box with sizes 2π and using $(N_x \times N_y \times N_z) = (512 \times 512 \times 512)$ collocation points, which is generated by instantaneously inserting a velocity field from a previously run DNS of forced isotropic turbulence into the middle of a field of zero initial velocity. As time progresses, the initial isotropic turbulence region spreads into the irrotational region in the absence of mean shear. The imposition of these initial boundary conditions can be accomplished by drastically reducing the time step in the simulations when the boundary condition is inserted, as described in Ref. 10. More details on this procedure can be found in Teixeira and da Silva[11] where a similar simulation is reported. In the present shear free simulation the Reynolds number based on the Taylor micro-scale is equal to $Re_\lambda \approx 115$ and the resolution is $\Delta x/\eta \approx 1.5$.

The other simulation used in this study is a DNS of a turbulent planar jet (labeled as $\text{PJET}_{chan.}$ in Taveira and da Silva[9]). The initial condition consists of interpolated velocity fields from a DNS of a turbulent channel flow and the computational domain extends to $(L_x, L_y, L_z) = (6.3H, 8H, 4.2H)$, where H is the inlet slot-width of the jet, along the streamwise (x), normal (y), and spanwise (z) jet directions, respectively, and the simulation uses $(N_x \times N_y \times N_z) = (1152 \times 1536 \times 768)$ grid points. At the far field self-similar region (where the subsequent analysis was carried out) the Reynolds number based on the Taylor micro-scale λ, and on the root-mean-square of the streamwise velocity u' is equal to $Re_\lambda = u'\lambda/\nu \approx 140$ across the jet shear layer and the resolution is $\Delta x/\eta \approx 1.1$.

The search for the VSL begins by re-analysing the mean profiles of several quantities conditioned in relation to the distance from the TNTI. These statistics have been used in many works and therefore the procedure to obtain them is only briefly described here.[1,3,12] The location of the TNTI is defined by the surface where the vorticity norm $\omega = (\omega_i\omega_i)^{1/2}$ is equal to a certain threshold $\omega = \omega_{tr}$, where the particular value of this threshold is obtained as described in Ref. 4. A local coordinate system located at the TNTI is then used to compute statistics as function of the distance to the TNTI location. In the resulting conditional mean profile the TNTI is located at $y_I = 0$, while the irrotational and turbulent regions are defined by $y_I < 0$ and $y_I > 0$, respectively.

Figure 1(a) shows mean profiles of enstrophy $\omega_i\omega_i/2$, enstrophy advection $u_j\partial/\partial x_j(\omega_i\omega_i/2)$, enstrophy production $\omega_i\omega_j s_{ij}$, and enstrophy viscous diffusion $\nu\partial^2/\partial x_j\partial x_j(\omega_i\omega_i/2)$ in relation to the distance to the TNTI (normalised by the Kolmogorov micro-scale η) for the planar jet configuration. The viscous diffusion exhibits a characteristic shape with positive/negative values near the TNTI, representing gain/loss of enstrophy, respectively,[2,4,12] and it is clear that this is the first term causing the observed enstrophy rise near the TNTI, in agreement with Corrsin and Kistler.[6] The enstrophy diffusion starts to be positive at $y_I/\eta \approx -2.0$ attaining its peak at $y_I/\eta \approx +2.5$ before decreasing to roughly zero at $y_I/\eta \approx +5.0$. The enstrophy production on the other hand only starts to be important once the TNTI has been crossed ($y_I/\eta > 0$) and is largely responsible for the enstrophy increase from that location onwards. An important point is reached by $y_I/\eta \approx +3.0$ when the enstrophy production surpasses the viscous diffusion. Similar conditional enstrophy budgets have been reported in a number of studies, e.g., Holzner *et al.*[2] and Taveira *et al.*[4] The interface region can then be divided into two sublayers:[5] the TSL with thickness δ_ω associated with the rapid vorticity rise, and the VSL with thickness δ_ν associated with the viscous diffusion of vorticity into the irrotational flow region.

By analysing Fig. 1(a) we can already deduce that the VSL is a very thin region indeed, making its detection very difficult. Moreover, presently no precise mathematical definition exists for this layer. We can however provide a definition based on the simple physical arguments put forward by Corrsin and Kistler.[6] If the VSL is a region dominated by viscous enstrophy diffusion and negligible enstrophy production we can define the following quantity as a criteria to detect the VSL:

$$\frac{|D_\omega|}{|P_\omega|} \geq r_{tr}, \tag{1}$$

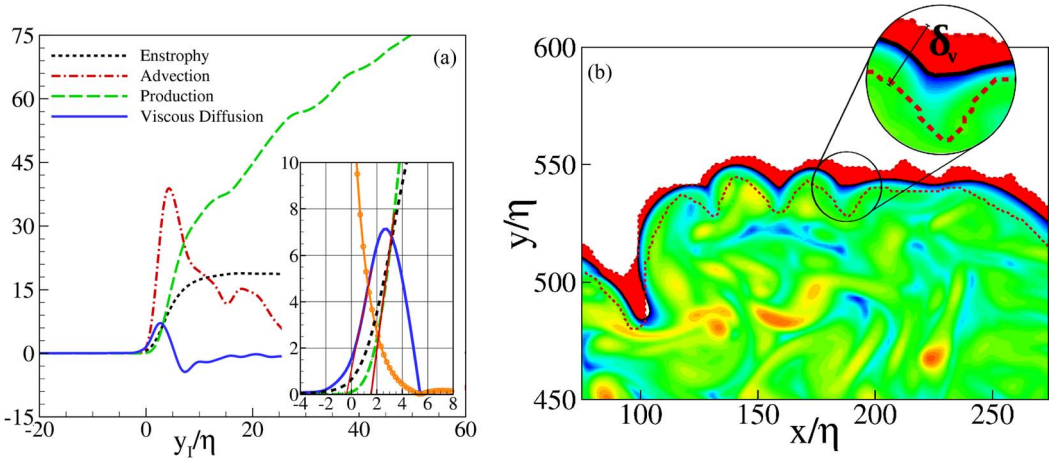

FIG. 1. (a) Conditional mean profiles as function of the distance from the TNTI for the turbulent planar jet: enstrophy $\omega_i\omega_i/2$, enstrophy advection $u_j\partial/\partial x_j(\omega_i\omega_i/2)$, enstrophy production $\omega_i\omega_j s_{ij}$, and enstrophy viscous diffusion $\nu\partial^2/\partial x_j\partial x_j(\omega_i\omega_i/2)$. The inset shows a zoom near the TNTI and the line with open circles (orange) represents the computed parameter r_{tr} defined by Eq. (1). (b) Contours of vorticity magnitude in a (x, y) plane near the TNTI in shear free turbulence. The dark line represents the TNTI location and the VSL defined through Eq. (1), with $r_{tr} = 2$ is represented in red. The inset shows the local VSL thickness.

where $D_\omega = \nu\partial^2/\partial x_j\partial x_j(\omega_i\omega_i/2)$, $P_\omega = \omega_i\omega_j s_{ij}$ are the diffusion and production terms from the enstrophy transport equation, and r_{tr} is a real number greater than 1. In the conditional mean profiles from Fig. 1(a) the VSL would be a layer extending from $y_I/\eta \approx -2.0$ to $y_I/\eta \approx +3.0$, i.e., a layer with roughly $\langle\delta_\nu\rangle/\eta \sim 5.0$. Indeed the thickness of the VSL judged from these conditional profiles and using the definition expressed in Eq. (1) is of the order of the Kolmogorov micro-scale as first suggested by Corrsin and Kistler.[6]

To detect the VSL we use the following procedure (see Fig. 1(b)): the 3D geometry of the VSL is detected using the definition of Eq. (1). Subsequently, for each (x, y) plane a centreline is defined along the entire VSL (both at the upper and lower shear layers of the jet and shear free turbulence simulations). This centreline is then used to define a local thickness of the VSL, δ_ν and the procedure is repeated for each other (x, y) plane. In the non-turbulent side both the diffusion and production decay extremely fast and we mark the outer edge of the VSL when their magnitude is less than 1% of their maximum irrotational far field values.

Figure 1(b) shows what to the authors knowledge is the first recorded visualisation of the VSL, together with the vorticity magnitude in a (x, y) plane near the TNTI in shear free turbulence. The VSL is here defined through Eq. (1) with $r_{tr} = 2$ and the VSL is represented as the layer existing between the two dashed (red) lines. As shown in this figure the VSL tends to form a thin continuous region bordering the entire external boundary of the TNTI, but it may appear to be fragmented at some regions along the TNTI for very high values of r_{tr}.

Figure 2(a) shows the mean value of the VSL thickness for both simulations used in the present work as function of the parameter r_{tr} for $1 \leq r_{tr} \leq 10$. Not surprisingly the mean thickness decreases as r_{tr} is increased, varying between $4.4 \leq \langle\delta_\nu\rangle/\eta \leq 7.3$ for shear free turbulence and $4.0 \leq \langle\delta_\nu\rangle/\eta \leq 6.2$ for the jet case, however the mean thickness seems to tend to a plateau and we can for the first time directly confirm the scaling law initially proposed by Corrsin and Kistler[6] for the mean thickness of the VSL: $\langle\delta_\nu\rangle \sim\eta$.

It is well known that the most intense vorticity structures (IVS) existing in a turbulent flow are well represented by a stable Burgers vortex (Jiménez and Wray[13]) and it has been recently shown that the same is true of the IVS bordering a TNTI (da Silva *et al.*[14]). Since the TNTI is partly formed around these IVS or "worms" it is tempting to explain the observed thickness of the VSL using the characteristics of small scale Burgers vortices near the TNTI, because these structures tend to be locally tangent to the TNTI,[15] and therefore the radial vorticity profile of these structures is preferentially "normal" to the local VSL position. In Ref. 8 the Burgers vortex (BV) was successfully

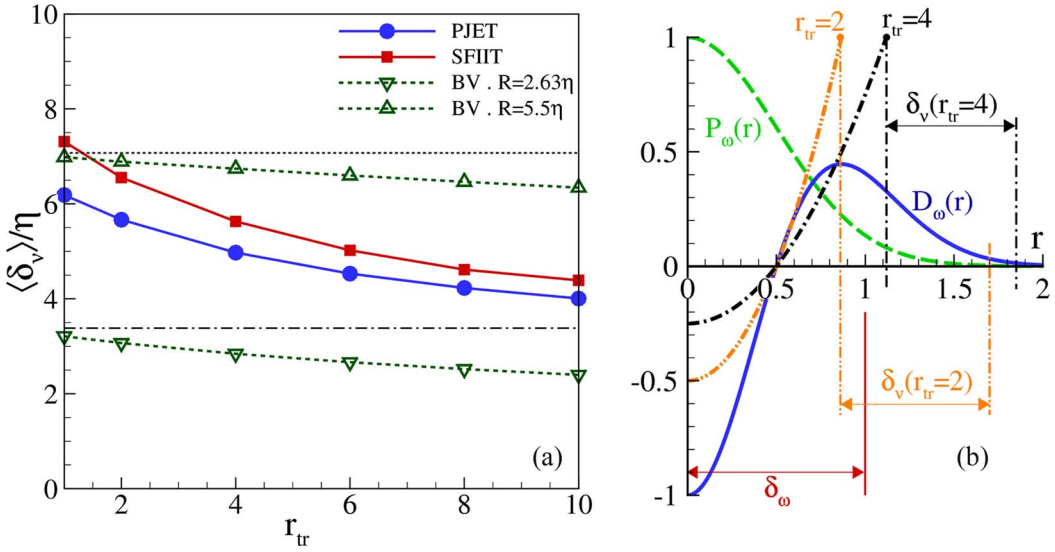

FIG. 2. (a) Mean VSL thickness $\langle\delta_\nu\rangle$ in shear free turbulence (SFT) and turbulent planar jet (PJET) for several values of the parameter r_{tr}, compared with the theoretical model based on a Burgers vortex (BV) for $f_\nu(r_0) = 0.99$. The line with triangles corresponds to $R/\eta = 5.5$ and inverted triangles to $R/\eta = 2.6$. The dashed and dashed-point horizontal lines correspond to $r_{tr} = 0$, $R/\eta = 5.5$, and $R/\eta = 2.6$, respectively. (b) Sketch of the analytical enstrophy production $P_\omega(r)$ and diffusion $D_\omega(r)$ for a Burgers vortex (normalised by their maxima). The TSL and VSL regions (with thicknesses δ_ω and δ_ν, respectively), and the parameter r_{tr} (for $r_{tr} = 2$ and $r_{tr} = 4$) are also shown.

used to study the thickness of the TSL region δ_ω (associated with the vorticity jump) observed in several flows. In the present work the BV is used to estimate the thickness of the VSL using Eq. (1). Figure 2(b) sketches the two sublayers within the TNTI, where the TSL is the inner layer at the core of the BV and the VSL is the viscous region at the outer edge of the BV.

In a stable Burgers vortex the axial, radial, and tangential velocities are given by $u_z(z) = \gamma_0 z$, $u_r(r) = -(\gamma_0/2)r$, and $u_\theta(r) = \omega_0[1 - exp(-r^2/R^2)]$, respectively, where γ_0 is a constant, $\omega_0 = \omega_z(r = 0)$ is the maximum vorticity, and $R = 2(\nu/\gamma_0)^{1/2}$ is the vortex core radius. Given that the radial vorticity profile is $\omega_z(r) = \omega_0 exp(-r^2/R^2)$, the enstrophy production is equal to $P_\omega(r) = \omega_0^2\gamma_0 exp(-2r^2/R^2)$ and the enstrophy diffusion is given by $D_\omega(r) = (2\nu\omega_0^2/R^2)(4r^2 - R^2)exp(-2r^2/R^2)$ it is possible to obtain an analytical expression for the parameter r_{tr} defined in Eq. (1) yielding $r_{tr} = (2\nu/\gamma_0 R^2)(4r^2 - R^2)$. This expression can now be used to compute the thickness of the VSL for a Burgers vortex. We define the function f_ν as the fraction of the total enstrophy diffusion, i.e., $f_\nu(r_0, \delta_B) = \int_{r_0}^{r_0+\delta_B} D_\omega(r)dr / \int_{r_0}^{\infty} D_\omega(r)dr$ where r_0 is the radial distance (from the center of the Burgers vortex) marking the beginning of the VSL, i.e., $D_\omega(r \geq r_0) \geq r_{tr}P_\omega(r)$, and δ_B is the associated thickness of the region dominated by enstrophy diffusion. For the Burgers vortex model this function is equal to

$$f_\nu(r_0, \delta_B) = 1 - \frac{exp\left[-2\delta_B\left(\delta_B + 2r_0\right)/R^2\right](\delta_B + r_0)}{r_0}. \tag{2}$$

Where r_0 is the radial distance (from the centre of the Burgers vortex) at which the diffusion is dominant. Naturally r_0 depends on the threshold value used to define the VSL r_{tr}. Particular solutions are $r_0 = R/2$ for $r_{tr} = 0$ and $r_0 = (R/2)\sqrt{1 + \gamma_0/(2\nu)}$ for $r_{tr} = 1$. In the present work we use $f_\nu(r_0, \delta_B) = 0.99$ (other values of f_ν give similar results). In order to compare the estimated δ_ν with the DNS results we need to link the Burgers vortex core radius to the Kolmogorov microscale. Using again the analytical Burgers model one can estimate the kinetic energy dissipation rate as $\varepsilon = 2\nu S_{ij}S_{ij} = 3\nu\gamma_0^2$ which yields $R/\eta \approx 2.63$. Results from DNS give $R/\eta \approx 5.5$ in isotropic turbulence,[13] and $R/\eta \approx 5.3$ in planar turbulent jets.[14] Figure 2(a) shows the mean VSL thickness as function of the parameter r_{tr} using the theoretical Burgers vortex model for both $R/\eta = 2.6$ and $R/\eta = 5.5$ and several values of the parameter r_{tr}. As can be seen the mean VSL thickness as measured

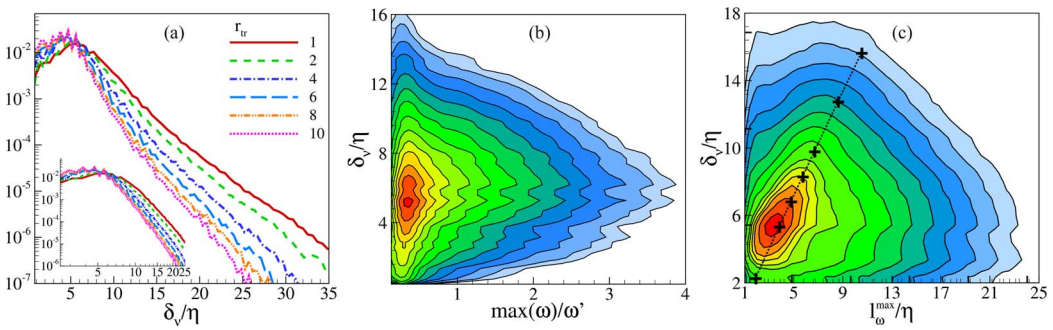

FIG. 3. (a) Probability density function (pdf) of the VSL thickness δ_v in the turbulent planar jet for several values of the parameter r_{tr}. (b) Joint probability density function (jpdf) between the local VSL thickness δ_v and the maximum vorticity magnitude $max(\omega)$ near the TNTI. (c) Joint probability density function (jpdf) between the local VSL thickness δ_v and the distance l_ω^{max} to the point of maximum vorticity magnitude. Both JPDFs are for the plane jet case with $r_{tr} = 1$. The results for the model based on the Burgers vortex are represented by crosses ("+") in Fig. 3(c).

from our DNS data is well within the theoretical estimates predicted for the VSL using the Burgers vortex model.

Figure 3(a) shows probability density functions (pdfs) of the local VSL thickness δ_v for the plane jet simulation as function from the parameter r_{tr}. The pdfs of δ_v/η display a large range of values which attests to the large variability of the local thickness. However, the shape of the pdf changes less for larger values of r_{tr}. A peak around $\delta_v/\eta \approx 5$ is visible which is indicative of the extremely small size of the VSL. The pdfs for the shear free turbulence case display a similar behaviour (not shown). The maximum detected values for the local δ_v are also similar in both flows, e.g., $max(\delta_v)/\eta \approx 32$ and $max(\delta_v)/\eta \approx 38$ for the jet and shear free case, respectively, for $r_{tr} = 10$.

The existence of a possible link between the VSL thickness and the neighbouring flow characteristics was studied by analysing joint probability density functions (jpdfs) between δ_v and the maximum vorticity magnitude $max(\omega)$ near the TNTI (see Figure 3(b)), and between δ_v and the distance from the maximum vorticity magnitude l_ω^{max} in the nearby flow region (Figure 3(c)). The figures are for the planar jet configuration and for $r_{tr} = 1$, but similar joint pdfs are recovered for the shear free case and the other values of r_{tr}.

No correlation can be observed between δ_v and $max(\omega)$, while δ_v and l_ω^{max} are clearly correlated for the most frequent, less intense values (e.g., $4 < \delta_v/\eta < 9$ and $2 < l_\omega^{max}/\eta < 7$), but not for the more intense and rare events (e.g., $\delta_v/\eta > 13$ and $l_\omega^{max}/\eta > 13$). It is not surprising that the present model for δ_v is unable to describe the entire VSL, as this figure shows, because the VSL is a continuous layer while the "worms" are located at a finite number of its "parts." The strong correlation observed for some values is however impressive because it suggests that the local VSL thickness is imposed by the eddies near the TNTI. Indeed the TNTI is (partially) defined by the outer boundary of the IVS,[14] and therefore in this case the distance from the VSL to the maximum local vorticity magnitude l_ω^{max} coincides roughly with the radius of the IVS: $R_{IVS} \sim l_\omega^{max}$. Since the IVS are well represented by Burgers vortices $R_{IVS} \approx R_{BV}$ the bigger vortices will exhibit a thicker VSL region surrounding them, which is precisely what is observed in Figure 3(c): higher local VSL thicknesses are associated with bigger local radius of the closest nearby IVS. The "crosses" in Figure 3(c) represent the (exact) relation between δ_v and the radius R_{BV} for a Burgers vortex, and as can be seen the slope for the model values follows very closely the relation between δ_v and l_ω^{max} directly computed from the DNS data.

Notice that this explanation is not inconsistent with the absence of correlation between δ_v and $max(\omega)$ displayed in Figure 3(b) because in a Burgers vortex the maximum vorticity is $\omega_0 = \Gamma/2\pi$ where Γ is the vortex circulation and is independent from the size of the vortex core radius R_{BV}. Finally, the lack of correlation observed for the more intense values of δ_v and l_ω^{max} (e.g., for $\delta_v/\eta > 13$) in Figure 3(c) can be explained by the contribution of the "incoherent" vorticity in defining the TNTI. It is possible also that this "incoherent" contribution may become more important in very

high Reynolds number flows, where the "fractal" aspects of the TNTI will emerge, however for the present flows and Reynolds numbers this simple model works very well.

In summary, DNS of planar jets and shear free turbulence give the first direct observation of the VSL defined by Corrsin and Kistler[6] as the layer at the edge of the TNTI where viscous diffusion dominates the mechanism of vorticity generation. The VSL is continuous across the TNTI with a local thickness exhibiting a large range of values but with a mean thickness which is of the order of the Kolmogorov micro-scale for both planar jets and shear free turbulence $\langle \delta_\nu \rangle / \eta \approx 4.0$–$7.3$. The results are consistent with the VSL being largely formed around the edge of IVS that are well modelled by a Burgers vortex, and demonstrates the existence of a connection between the local VSL thickness and the nearby turbulent flow characteristics, i.e., the size of the IVS near the VSL imposes its local thickness.

Rodrigo Taveira acknowledges support from the Portuguese Foundation for Science and Technology under Grant No. BPD/47815/2008.

[1] D. K. Bisset, J. C. R. Hunt, and M. M. Rogers, "The turbulent/non-turbulent interface bounding a far wake," J. Fluid Mech. **451**, 383–410 (2002).
[2] M. Holzner, A. Liberzon, N. Nikitin, W. Kinzelbach, and A. Tsinober, "Small-scale aspects of flows in proximity of the turbulent/nonturbulent interface," Phys. Fluids **19**, 071702 (2007).
[3] J. Westerweel, C. Fukushima, J. M. Pedersen, and J. C. R. Hunt, "Momentum and scalar transport at the turbulent/non-turbulent interface of a jet," J. Fluid Mech. **631**, 199–230 (2009).
[4] R. R. Taveira, J. S. Diogo, D. C. Lopes, and C. B. da Silva, "Lagrangian statistics across the turbulent-nonturbulent interface in a turbulent plane jet," Phys. Rev. E **88**, 043001 (2013).
[5] C. B. da Silva, J. C. R. Hunt, I. Eames, and J. Westerweel, "Interfacial layers between regions of different turbulent intensity," Annu. Rev. Fluid Mech. **46**, 567–590 (2014).
[6] S. Corrsin and A. L. Kistler, "Free-stream boundaries of turbulent flows," Technical Report TN-1244, NACA, 1955.
[7] B. R. Morton, "The generation and decay of vorticity," Geophys. Astrophys. Fluid Dynamics **28**, 277–308 (1984).
[8] C. B. da Silva and R. R. Taveira, "The thickness of the turbulent/nonturbulent interface is equal to the radius of the large vorticity structures near the edge of the shear layer," Phys. Fluids **22**, 121702 (2010).
[9] R. R. Taveira and C. B. da Silva, "Kinetic energy budgets near the turbulent/nonturbulent interface in jets," Phys. Fluids **25**, 015114 (2013).
[10] B. Perot and P. Moin, "Shear-free turbulent boundary layers. Part 1. Physical insights into near-wall turbulence," J. Fluid Mech. **295**, 199–227 (1995).
[11] M. A. C. Teixeira and C. B. da Silva, "Turbulence dynamics near a turbulent/non-turbulent interface," J. Fluid Mech. **695**, 257–287 (2012).
[12] C. B. da Silva and J. C. F. Pereira, "Invariants of the velocity-gradient, rate-of-strain, and rate-of-rotation tensors across the turbulent/nonturbulent interface in jets," Phys. Fluids **20**, 055101 (2008).
[13] J. Jiménez and A. Wray, "On the characteristics of vortex filaments in isotropic turbulence," J. Fluid Mech. **373**, 255–285 (1998).
[14] C. B. da Silva, R. J. N. dos Reis, and J. C. F. Pereira, "The intense vorticity structures near the turbulent/non-turbulent interface a jet," J. Fluid Mech. **685**, 165–190 (2011).
[15] C. B. da Silva and R. J. N. dos Reis, "The role of coherent vortices near the turbulent/non-turbulent interface in a planar jet," Philos. Trans. R. Soc. A **369**, 738–7531 (2011).